J Wood Sci (2006) 52:377–382
DOI 10.1007/s10086-005-0786-8

ORIGINAL ARTICLE

Tomokazu Sasaki · Tetsuaki Okamoto
Gyosuke Meshitsuka

Influence of deformability of kraft pulp fiber surface estimated by force curve measurements on atomic force microscope (AFM) contact mode imaging

Received: May 20, 2005 / Accepted: November 9, 2005 / Published online: April 28, 2006

Abstract Attempts were made to obtain high-resolution images of an unbeaten bleached softwood kraft pulp fiber surface in water by applying contact mode atomic force microscopy. However, clear topographic images could not be obtained. In order to investigate the possibility of deformation of a pulp fiber surface during scanning, force curve measurements were applied to pulp fiber surfaces. It was found that a pulp fiber in water had a more deformable surface than an air-dried pulp fiber in air. Moreover, the spring constant of it was estimated to be close to that of a cantilever applied for imaging. Therefore, the images of a pulp fiber surface in water were thought to be significantly affected by deformation, which was considered to be an important cause of the unclear images.

Key words Atomic force microscopy · Force curve measurement · Kraft pulp fiber · Pulp fiber in water

Introduction

It is well known that fibrils, which have nanometer-scale architectures, exist on a kraft pulp fiber. However, their detailed structures are still unknown, mainly because few methods are available for investigation. The ultimate aim of this study is to understand detailed structures of fibrils on kraft pulp fibers, and at the same time, because pulp fibers are materials of paper, the authors would like to obtain beneficial information to understand fiber–fiber bonding on a nanometer scale.

Atomic force microscopy (AFM), which has been developed in recent years has resolution as high as that of electron microscopy, and has the potential to analyze nanometer-scale architectures.[1] AFM has great advantages over electron microscopy in that nonconductive samples can be observed directly not only in air but also in liquid.

Many research groups have reported about AFM imaging of biological samples in air. Thalhammer et al.[2] showed high resolution images of human metaphase chromosomes and Kirby et al.[3] obtained clear images of water chestnut cell walls. These imagings were conducted by contact mode AFM, where a tip of a cantilever scans a sample in contact with its surface. Cyclic contact mode has recently developed, in which less force is considered to be exerted by a tip to a sample surface during imaging. This mode is, therefore, thought to be suitable for imaging deformable samples such as proteins. For example, Yamaguchi et al.[4] applied this imaging mode for dimeric DNA catenanes in air and obtained clear images. Curdlan, which is microbial fermentation extracellular polymer, was analyzed by Ikeda et al.[5] to give clear images of Curdlan and its microgel by cyclic contact mode.

Clear images of biological samples could be also obtained in liquid environment. Hansma et al.[6] obtained clear images of plasmid DNA in propanol by the contact mode, and Hallett et al.[7] reported high resolution images of myosin and titin protein in propanol by both contact mode and cyclic contact mode. Tamayo[8] showed detailed structures of human chromosomes in phosphate-buffered saline solution by cyclic contact mode imaging. However, high resolution images of biological samples with rough and/or deformable surfaces such as a living bacterium and an intact plant cell, could not be always obtained even by cyclic contact mode imaging.[9–11] This may be due to the difficulties in adjusting

T. Sasaki (✉) · G. Meshitsuka
Laboratory of Wood Chemistry, Department of Biomaterial Sciences, Graduate School of Agricultural and Life Sciences, The University of Tokyo, 1-1-1 Yayoi, Bunkyo-ku, Tokyo 113-8657, Japan
Tel. +81-3-5841-5264; Fax +81-3-5802-8862
e-mail: musigny0610@hotmail.com

T. Okamoto
Department of Physics, School of Science and Engineering, Waseda University, Tokyo 171-0033, Japan

Parts of this article were presented at the 53rd Annual Meeting of the Japan Wood Research Society, Fukuoka, Japan, March 2003, the 54th Annual Meeting of the Japan Wood Research Society, Hokkaido, Japan, August 2004, the 12th International Symposium on Wood and Pulping Chemistry, Madison, USA, June 2003, and the 13th International Symposium on Wood, Fiber and Pulping Chemistry, Oakland, New Zealand, May 2005

imaging parameters for rough and/or deformable sample surfaces in liquid.

In the case of imaging a pulp fiber surface, which is a biological sample with a rough surface, clear images could be obtained in air by both contact mode and cyclic contact mode. Okamoto and Meshitsuka[12] showed clear images of a kraft pulp fiber surface by the contact mode. By cyclic contact mode imaging, Gustafsson et al.[13] reported high resolution images of the surface of thermomechanical pulp fibers, and Niemi et al.[14] and Simola et al.[15] also showed clear images of fibrils on the surface of kraft pulp fibers. There are only a few reports of surface structures of kraft pulp fibers in water by contact mode AFM. Pang and Gray[16] reported that microfibrils were observed in some area on a beaten bleached softwood kraft pulp fiber. AFM observation of an unbeaten unbleached softwood kraft pulp fiber in water was performed by Hanley and Gray[17] These images were much less clear than those obtained in air.

Force curve measurement is another function of AFM, and various physical properties of the imaging area of a sample surface can be obtained by use of the measurement.[10,11] In the paper and pulping science field, Furuta and Gray[18] have applied force curve measurement to dissolving-grade softwood sulphite pulp fibers in deionized water, and discussed their surface properties.

In this study, the deformability of kraft pulp fibers in air and water was determined by force curve measurement, and the relationship between the deformability and the clarity of AFM images of kraft pulp fibers is discussed.

Materials and methods

Sample preparations

Never-dried unbeaten bleached softwood kraft pulp fibers (Oji Paper, Kasugai Mill) were used in this study. The fibers were washed with deionized water until the filtrate was almost neutral, and then dried by two different drying methods. One method was air drying where pulp fibers were dried overnight under ambient conditions to prepare air-dried pulp fibers (AD pulp fibers). The other drying method was critical point drying. The detailed procedures of this method are as follows. After stepwise solvent exchange of pulp fibers from deionized water to ethanol, the pulp fibers were suspended in ethanol and set in a critical point dryer (Hitachi HCP-2), and then immersed in liquid CO_2. They were dried at 31°C through supercritical fluid to prepare critical point-dried pulp fibers (CPD pulp fibers).

The less twisted fibers were selected, and attached to steel disks with double-sided adhesive tape. Both types of dried pulp fibers were set on the sample stage, then observed in air by AFM. Some AD pulp fibers on steel disks were directly immersed in ultra pure water, and used for AFM observation.

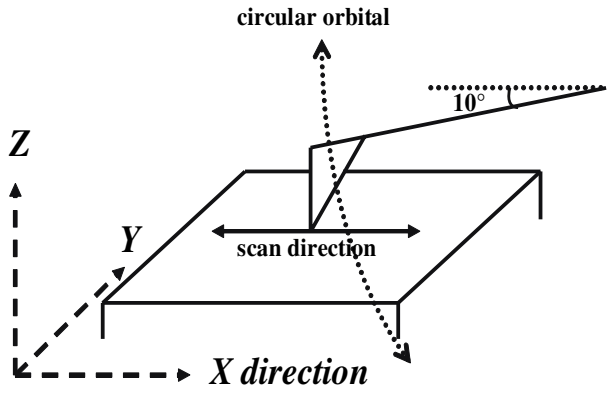

Fig. 1. Schematic illustration of an orbit of a tip of a cantilever on an atomic force microscope

AFM observation

AFM (Shimadzu SPM-9500) was used for observations at room temperature under the constant force mode of contact. Schematic illustration of AFM is shown in Fig. 1, where the *X* direction is parallel to the scan direction, the *Y* direction is perpendicular to the scan direction, and the *Z* direction is perpendicular to the *XY* plane. An advantage of contact mode is that the same cantilever can be applied for imaging and force curve measurements. (Generally, spring constants of cantilevers for cyclic contact mode in air are too large for investigating deformability of kraft pulp fiber surfaces by force curve measurements.) Short cantilevers (OMLC-TR400PSA) of 100 μm long in length, whose nominal spring constant was about 0.1 N/m, were used. Cantilevers with small curvature radius at their tips were selected and applied to imaging and to force curve measurement. Electrostatic effect was eliminated from samples and cantilevers by the use of an ionized air blower (model-10/10 Hugle Electronics) before imaging. Topographic trace and retrace images were obtained. Scan size and scan speed were 1 μm × 1 μm (512 pixel × 512 pixel) and 1.0–1.2 Hz, respectively. The scan direction was perpendicular to the pulp fiber axis. The force exerted by a tip to a sample surface was controlled to be as small as possible during imaging by adjusting the operating point (the set point). Topographic images were modified with X-line offset and plane-fitting. Correlation coefficients of topographic profiles of trace and retrace images were calculated after each topographic retrace profile was shifted in the *Y* direction in order to obtain the highest correlation coefficients.

AFM force curve measurement

After finding "horizontal area" (defined as an area where the angle between the normal line of the approximated plane of the AFM image and *Z* axis is small) via imaging, force curve measurements were carried out on 10 to 20 random points in the area. Most of the angles of imaging area were less than 10°. Force curve measurements were subsequently carried out on a cleaved mica plate under the

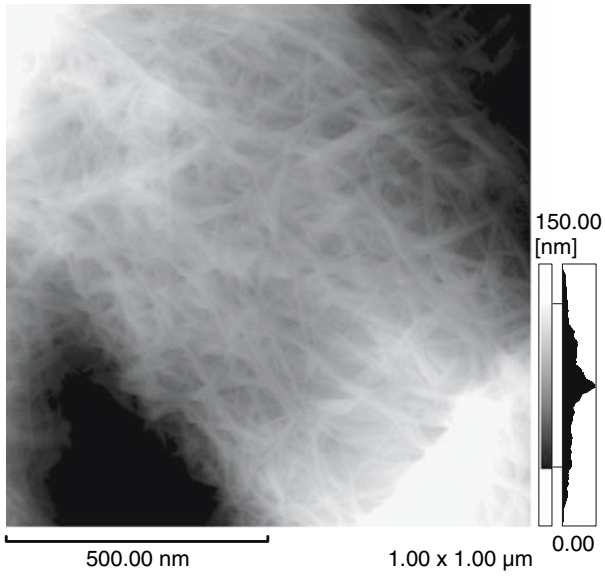

Fig. 2. Atomic force microscope (AFM) trace image of an air-dried (AD) pulp fiber surface in air

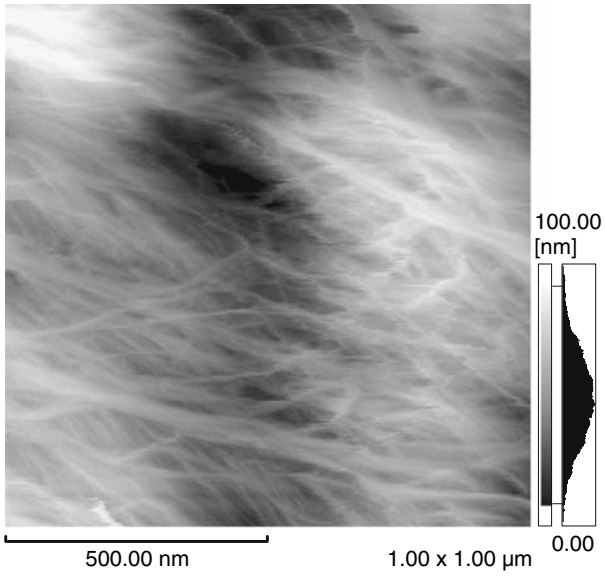

Fig. 3. AFM trace image of an AD pulp fiber surface in water

same atmosphere, with the same laser spot position at the back of a cantilever, because a slope of a force curve on the same position changed depending on the laser spot position at the back of a cantilever. A cleaved mica plate was used as a hard sample, for which the deformation was thought to be undetectable by the measurements. The speed of the sample stage lifted in the Z direction was about 300–600 nm/s. Slopes of force curves were calculated by the root mean square until the sample stage was lifted by 20 nm after a sample surface was contacted by a tip. By comparing slopes of force curves for a pulp fiber with those for a mica plate, the extent of deformation of pulp fiber surfaces in the Z direction was calculated.

Results and discussion

Clarity of AFM images

A clear topographic image of an AD pulp fiber surface in air could be obtained as shown in Fig. 2, and fibrils of an AD pulp fiber surface could be observed as reported in the previous AFM observations.[12–15] On the other hand, each fibril of an AD pulp fiber surface in water was not clear, although fibrils could be recognized in the image as shown in Fig. 3.

Deformation during scanning was expected to be a cause of the low clarity. There are two types of deformation, one is irreversible deformation and the other is reversible. In order to investigate the influence of irreversible deformation on clarity, scans in the X direction without shifting in the Y direction were repeated in the imaging of a pulp fiber surface in water. Then, correlation coefficients between the first trace line and the following trace lines were high and almost constant; the correlation coefficients between the first and second trace lines, between the first and fifth trace lines, and between the first and tenth trace lines were 0.997, 0.998, and 0.998, respectively. Irreversible deformation was, therefore, very low during imaging in this observation condition. For investigation of reversible deformation, force curve measurement was examined.

Development of force curve measurement for kraft pulp fiber surfaces

Force curve measurement records the motion of a tip of a cantilever relative to the vertical movement of the sample stage. In other words, force curve measurement enables us to know the moving distance of a tip in the Z direction when the sample stage is lifted by a constant distance.

Figure 4 shows typical force curves of an AD pulp fiber surface in air, a CPD pulp fiber surface in air, an AD pulp fiber surface in water, and a cleaved mica surface in both air and water. In general, force curve slopes on pulp fiber surfaces obtained in this study could be regarded as straight lines. This means that deformation of pulp fiber surface measured by force curves in our conditions could be thought of as elastic deformation. In other words, the pulp fiber surface could be considered to be a spring against the force in the Z direction during our force curve measurements.

Figure 5a shows force curve slopes of AD pulp fiber surface in air, CPD pulp fiber surface in air, an AD pulp fiber surface in water, and a cleaved mica surface in both air and water. Some values are found to be much larger than 1 nm/nm in the case of the AD pulp fiber surface in air. This means that a tip was lifted by much more than 1 nm with the stage lifted by 1 nm. These values seemed to be abnormal, and attempts to interpret them are outlined in the following discussion.

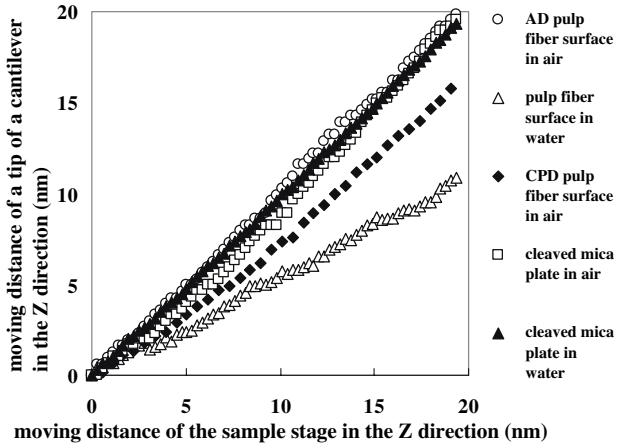

Fig. 4. Typical force curves of an AD pulp fiber surface in air, a critical point-dried (CPD) pulp fiber surface in air, an AD pulp fiber surface in water, a cleaved mica plate in air, and a cleaved mica plate in water. The curves were taken during approach. Zero on the *X* axis of the figure refers to initial contact of tips of cantilevers to the sample surfaces

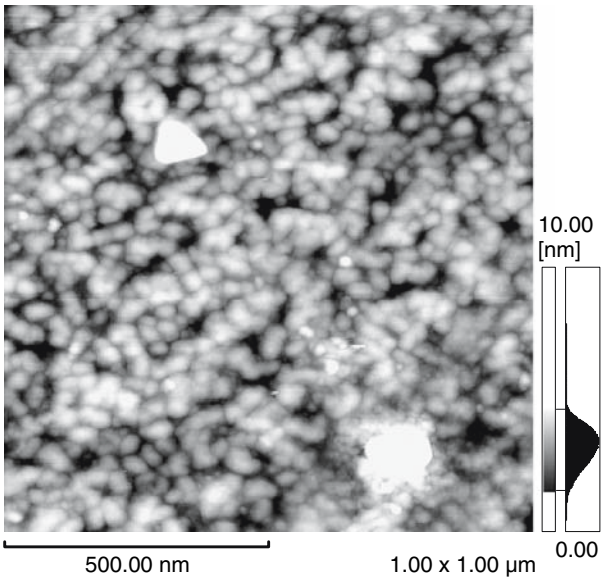

Fig. 6. AFM trace image of a niobium metal plate in air

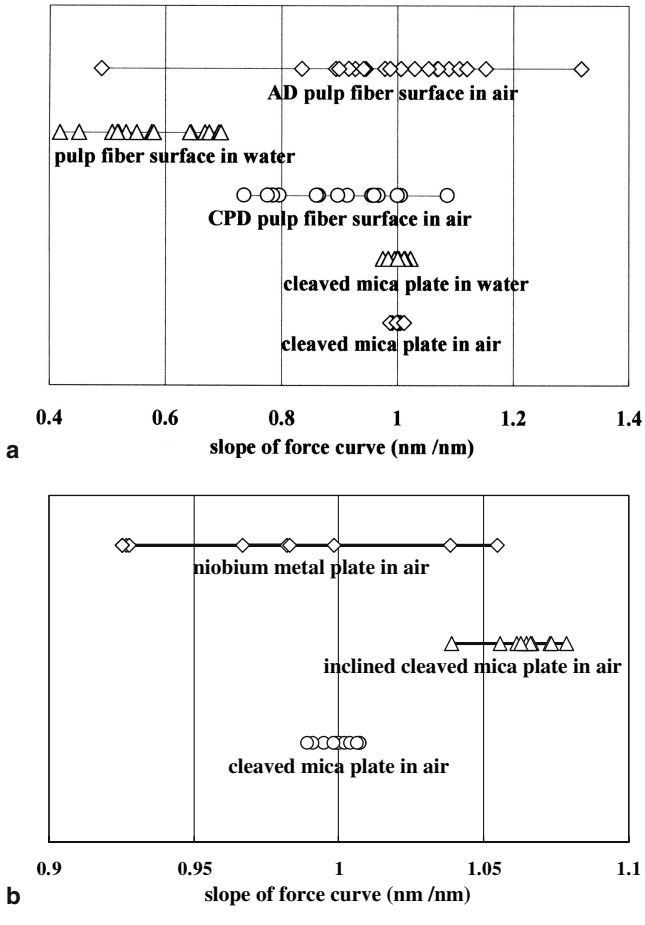

Fig. 5a, b. Force curve slopes of **a** an AD pulp fiber surface in air, a CPD pulp fiber surface in air, an AD pulp fiber surface in water, a cleaved mica plate in air, a cleaved mica plate in water, and **b** a niobium metal plate in air, a horizontal (noninclined) cleaved mica plate in air, and an inclined cleaved mica plate in air

Figure 5b shows the force curve slopes of a niobium metal plate in air and Fig. 6 shows its image. The niobium metal plate had to be as hard as a mica plate, and the extent of deformation of its surface should be smaller than the detection limit in the force curve measurement. Some abnormal values were also observed in the slopes of a niobium metal plate.

Because a tip moves along a circular orbit during force curve measurement and the cantilever is at 10° relative to the *X* axis as shown in Fig. 1, the contact point of a tip to a sample surface was expected to be shifted largely in the *X* direction when a cantilever was deflected. In order to confirm this, force curve measurements were made for an inclined mica plate whose gradient was negative in the *X* direction. As shown in Fig. 5b, the slopes of force curves for the inclined cleaved mica plate were found to be larger than those of a noninclined cleaved mica plate. When the stage was lifted in the *Z* direction by 20 nm, the shift of the contactpoint in the *X* direction on a horizontal and flat surface was 3.5 nm ideally. In the case of the mica plate whose gradient was –0.27 in the *X* direction, the moving distance of a tip in the *Z* direction was estimated to be 1.09 nm ideally when the stage was lifted by 1 nm. The ideal value was close to the actual value of 1.07 nm. Therefore, it was reasonable to say that a tip climbed up a gradient of the inclined mica plate as the stage was lifted, and consequently slopes of force curves larger than 1 nm/nm were observed. So, it is strongly suggested that samples with surface slopes give incorrect results in force curve measurement.

A cleaved mica plate is known to have a flat surface in the atomic level, but the niobium metal plate surface is covered with unevenness from the scale of several nanometers to several tens of nanometers as shown in Fig. 6. For this reason, it was thought that abnormal values were observed in the results of force curve measurements for the niobium metal plate. Each slope of a force curve contains

not only the information of the deformability of a sample surface but also the influence of the gradient of a sample surface.

Surfaces of kraft pulp fibers are covered with the roughness from the scale of hundreds of nanometers to several micrometers. Moreover, the roughness is covered with architectures from the scale of several nanometers to tens of nanometers. When the deformability of a kraft pulp fiber surface with these features is examined by force curve measurements, it is important to select a "horizontal area" on a pulp fiber surface and to measure as many points as possible inside the area. It is considered that the average of multipoint force curve measurements on a "horizontal area" should be quite close to the true value representing deformability of a kraft pulp fiber surface.

Z Axis deformability of kraft pulp fiber surfaces

The *Z* axis deformability value of a pulp surface could be written as follows.

$$d = 1 - s$$

where d is the *Z* axis deformability value of a sample by the force curve measurement (nm/nm), and s is the average of the force curve slopes on a sample (nm/nm)

The *Z* axis deformability value of the AD pulp fiber surfaces in air was found to be near 0 nm/nm. The *Z* axis deformability value of the AD pulp fiber surface in water was found to be 0.4 nm/nm. This means that an AD pulp fiber surface in water has a more deformable feature in the *Z* axis than an AD pulp fiber surface in air.

Critical point drying is generally believed to be a method with little force during the drying process, and is often applied for the preparation of biological samples for scanning electron microscopy (SEM) observations.[19,20] AFM observations of CPD pulp fiber surfaces in air were, therefore, expected to give us some characteristics of pulp fiber surfaces in water. An AFM image of a CPD pulp fiber surface in air is shown in Fig. 7, and fibrils can be observed in the image as well. By the force curve slopes as shown in Fig. 5a, the *Z* axis deformability value of the CPD pulp fiber surface in air was found to be 0.1 nm/nm. This value means that a CPD pulp fiber surface in air was more deformable in the *Z* direction than an AD pulp fiber surface in air, although it was less deformable than an AD pulp fiber surface in water.

The *Z* axis spring constant could be obtained by the *Z* axis deformability value and the spring constant of the cantilever.

$$k_s = \frac{1-d}{d} k_c$$

where k_s is a *Z* axis spring constant of a sample surface (N/m), k_c is a nominal spring constant of a cantilever which was about 0.1 N/m in this study (N/m), and d is the *Z* axis deformability value of a sample (nm/nm).

In the case of an AD pulp fiber surface in air, the *Z* spring constant was calculated to be much larger than that of a cantilever. (However, due to this hardness, its spring constant could not be accurately determined.) In contrast, a *Z* axis spring constant of an AD pulp fiber surface in water was found to be close to that of a cantilever. The *Z* axis spring constant of a CPD pulp fiber surface in air was calculated to be several times larger than that of a cantilever, and was between that of an AD pulp fiber surface in air and that of an AD pulp fiber surface in water.

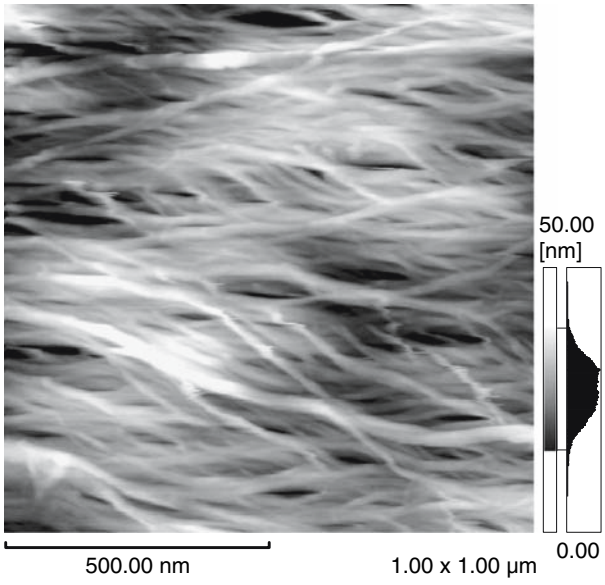

Fig. 7. AFM trace image of a CPD pulp fiber surface in air

Deformation in the *Z* direction ought to affect contact mode imaging, and this deformation should reduce the resolution of images. In addition, a deformable structure in the *Z* direction is expected to be deformable in the *X* and *Y* directions as well.

Influence of deformability of kraft pulp fiber surfaces to AFM imaging

If a deformation in the *Z* and/or *X* direction (the scanning direction) occurs during imaging, the identity of the trace and retrace image should be decreased. Here, trace image means an image obtained by scanning a sample surface in the $+X$ direction. A retrace image means an image by scanning the same area in the opposite direction. Correlation coefficients of topographic profiles between trace and retrace images (Ctr) could give an evaluation for identity of trace and retrace images (Fig. 8).

The average of Ctr of a niobium metal plate, which was expected to have a hard surface, was 0.998 (in air), and that of an AD pulp fiber in air was almost the same as that of a metal plate (0.997). In contrast, the average of Ctr of an AD pulp fiber in water (0.949) was lower than that of a metal plate. In addition, the average of Ctr of a CPD pulp fiber in air (0.963) was found to be between that of an AD pulp fiber in air and that in water. This means that Ctr is correlated with *Z* axis spring constant of kraft pulp fiber surfaces. The lower *Z* axis spring constant of an AD pulp fiber surface in

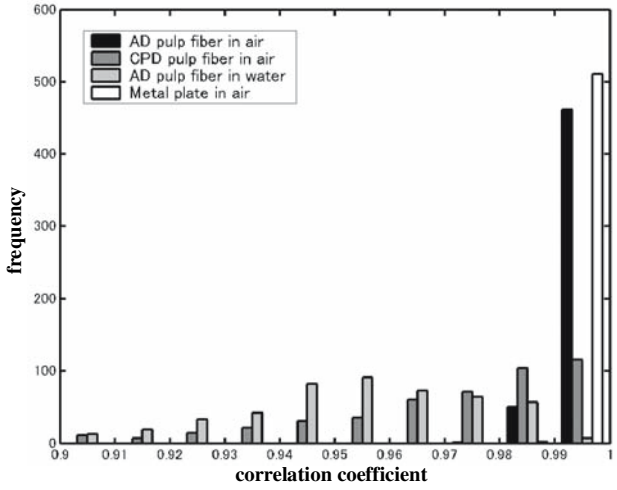

Fig. 8. Correlation coefficients of 512 topographic profiles between trace and retrace images of AD pulp fiber surfaces both in air and water, a CPD pulp fiber surface in air, and a niobium metal plate in air

water (which was almost the same as that of the cantilever used in this study) resulted in a larger sample deformation in the Z and/or X direction during imaging.

This deformation should reduce the AFM image clarity. A few methods are, therefore, expected to be beneficial to observe deformable kraft pulp fiber surfaces in water. One is the application of cantilevers with a smaller spring constant. AFM cyclic contact mode seems to be useful because the mode is generally said to be effective for the observation of soft samples such as proteins. Another possible method may be to solidify a sample surface by some kind of chemical treatment.

Conclusions

1. The AFM imaging clarity of kraft pulp fiber surfaces was found to be different depending on imaging environments (in air or water) and/or drying methods. The order of clarity was as follows (from highest to lowest): an AD pulp fiber in air, a CPD pulp fiber in air, and an AD pulp fiber in water.
2. By force curve measurements, an AD pulp fiber in water was found to have a more deformable surface in the Z direction than an AD pulp fiber in air. A CPD pulp fiber in air was also found to have a more deformable surface in the Z direction than an AD pulp fiber in air, but a less deformable surface in the Z direction than an AD pulp fiber in water.
3. Correlation coefficients of topographic profiles between trace and retrace images of an AD pulp fiber surface in water tended to be lower than those of an AD kraft pulp fiber surface in air. Correlation coefficients between trace and retrace images of a CPD pulp fiber surface in air also tended to be between those of an AD pulp fiber surface in air and an AD pulp fiber surface in water.
4. The lower Z axis spring constant of an AD pulp fiber surface in water (which was almost the same as that of the cantilever used in this study) resulted in a larger deformation of a sample surface in the Z and/or X direction during imaging. This deformation should reduce AFM image clarity.

References

1. Binnig G, Quate CF, Geber CH (1986) Atomic force microscope. Phys Rev Lett 56:930
2. Thalhammer S, Koehler U, Stark RW, Heckl WM (2000) GTG banding pattern on human metaphase chromosomes revealed by high resolution atomic-force microscopy. J Microsc 202:464–467
3. Kirby AR, Gunning AP, Waldron KW, Morris VJ, Ng A (1996) Visualization of plant cell walls by atomic force microscopy. Biophys J 70:1138–1143
4. Yamaguchi H, Kubota K, Harada A (2000) Direct observation of DNA catenanes by atomic force microscopy. Chem Lett 4:384–385
5. Ikeda S, Shishido Y (2005) Atomic force microscopy studies on heat-induced gelation of Curdlan. J Agric Food Chem 53:786–791
6. Hansma HG, Vesenka J, Siegerist C, Kelderman G, Morrett H, Sinsheimer RL, Elings V, Bustamante C, Hansma PK (1992) Reproducible imaging and dissection of plasmid DNA under liquid with the atomic force microscope. Science 256:1180–1184
7. Hallett P, Tskhovrebova L, Trinick J, Offer G, Miles MJ (1996) Improvements in atomic force microscopy protocols for imaging fibrous proteins. J Vac Sci Technol B 14:1444–1448
8. Tamayo J (2003) Structure of human chromosomes studied by atomic force microscopy. J Struct Biol 141:198–207
9. Vié V, Giocondi MC, Lesniewska E, Finot E, Goudonnet JP, Grimellec CL (2000) Tapping-mode atomic force microscopy on intact cells: optimal adjustment of tapping conditions by using the deflection signal. Ultramicroscopy 82:279–288
10. Callow JA, Crawford SA, Higgins MJ, Mulvaney P, Wetherbee R (2000) The application of atomic force microscopy to topographical studies and force measurements on the secreted adhesive of the green alga *Enteromorpha*. Planta 211:641–647
11. Velegol SB, Logan BE (2002) Contributions bacterial surface polymers, electrostatics, and cell elasticity to the shape of AFM force curves. Langmuir 18:5256–5262
12. Okamoto T, Meshitsuka G (1999) Interpretation of AFM image of kraft pulp. Proc 10th ISWPC, Yokohama, Japan 3:154–157
13. Gustafsson J, Lehto JH, Tienvieri T, Ciovica L, Peltonen J (2003) Surface characteristics of thermomechanical pulps; the influence of defibration temperature and refining. Colloid Surface A 225:95–104
14. Niemi H, Paulapuro H, Mahlberg R (2002) Application of scanning probe microscopy to wood, fibre and paper research. Pap Puu-Pap Tim 84:389–406
15. Simola J, Malkavaara P, Alén R, Peltonen J (2000) Scanning probe microscopy of pine and birch kraft pulp fibres. Polymer 41:2121–2126
16. Pang L, Gray DG (1998) Heterogeneous fibrillation of kraft pulp fibre surfaces observed by atomic force microscopy. J Pulp Pap Sci 24:369–372
17. Hanley SJ, Gray DG (1999) AFM images in air and water of kraft pulp fibers. J Pulp Pap Sci 25:196–200
18. Furuta T, Gray DG (1998) Direct force-distance measurements on wood-pulp Fibres in aqueous media. J Pulp Pap Sci 24:320–324
19. Tay FR, Pang KM, Gwinnett AJ, Wei SHY (1994) A scanning electron microscopic study of the extent of resin penetration into human coronal dentin following a total etch technique in vivo. Cell Mater 4:317–329
20. Sutton NA, Hughes N, Handley PS (1994) A comparison of conventional SEM techniques, low temperature SEM and the electronscan wet scanning electron microscope to study the structure of a biofilm of *Streptococcus crista* CR3. J Appl Bacteriol 76:446–454